

# Electronic Supplementary Information

## Recognition of Carbon Nanotube Chirality by Phage Display

Ting Yu<sup>a</sup>, Yingxue Gong<sup>b</sup>, Tingting Lu<sup>a</sup>, Li Wei<sup>a</sup>, Yuanqing Li<sup>a</sup>, Yuguang Mu<sup>c</sup>, Yuan Chen<sup>a</sup> and Kin Liao<sup>\*a</sup>

a School of Chemical and Biomedical Engineering, Nanyang Technological University, Singapore. Fax: +65 6791 6905; Tel: +65 6790 5835; E-mail: askliao@ntu.edu.sg

b Research Centre for Molecular Biology, Institute of Life and Health Engineering, College of Life Sciences and Technology, Jinan University, Guangzhou, P. R. China

c School of Biological Sciences, Nanyang Technological University, Singapore.

### Experimental Methods

#### Titering

Titering is a process to quantify phage. We used ER2738 as *E. coli* host strain, which is a *lacZα*-absent strain for blue-white screen. Before infection, we inoculate 5 ml of LB medium with a single colony of ER2738 with shaking at 37°C until mid-log phase ( $OD_{600} \sim 0.5$ ). At that time, 200  $\mu$ l of bacteria was dispensed into individual microcentrifuge tubes. 10  $\mu$ l of 10-fold serial phage dilutions was used to infect the host strain prepared. The infected bacteria were added into 3 ml melt agarose top in a Falcon tube and then the mixture was vortexed and poured onto an LB/IPTG/Xgal plate. These plates contain a combination of IPTG (isopropyl  $\beta$ -D-thiogalactoside) and Xgal (5-Bromo-4-chloro-3-indolyl- $\beta$ -D-galactoside) which produce a blue color

in the presence of  $\Delta(lacZ\alpha)$  bacteria infected by the modified M13 phage which carry the *lacZ* $\alpha$  gene. Therefore, incubation of the plates at 37°C resulted in the appearance of blue plaques, indicating where engineered M13 phage, not the wild-type phage, had successfully infected a colony. The plaques on plate having 50 ~ 200 plaques were counted. Phage concentration is calculated by the following formula in *plaque forming units* (pfu).

$$\text{Phage concentration} = \frac{\text{the number of plaques}}{10^{\text{dilution factor}}} \text{ (pfu/ml)}$$

### **Characterization of Binding Clones**

Phages from monoclonal were amplified in order to provide sufficient phage DNA for sequencing. 2 ml 1:10 dilution of an overnight *E.coli* ER2738 culture was dispensed into 15 ml centrifuge tubes, one for each clone to be characterized. The eluted phage in the sixth round didn't undergo further amplification and proper phage dilution was prepared to ensure that, after titering, the plates had no more than 100 blue plaques. Well-separated blue plaques were isolated and transferred to tubes containing diluted ER2738 culture. The cultures were incubated at 37°C with harsh agitation for 4.5 hours.

Cultures were then transferred into 2ml microcentrifuge tubes and bacteria were removed by centrifugation at 10,000g for 15 minutes. Phage in the top 200  $\mu$ l supernatant was 1:1 diluted with sterile glycerol and stored at -20°C for further applications. The upper 1200  $\mu$ l supernatant was transferred to a fresh microcentrifuge tube without disturbing the bacterial pellet. A second centrifugation step was always performed to ensure a clean supernatant fraction with no bacterial carryover. The phage DNA isolation was accomplished by the use of QIAprep Spin

M13 Kit (QIAGEN, Germany). Phage DNA was quantified on either a BioPhotometer (Eppendorf, Germany) or a NanoDrop ND-1000 spectrophotometer (NanoDrop Technologies, Inc., USA). 50 - 100 ng of DNA was submitted to sequencing facilities (either Research Biolabs Pte Ltd, Singapore, or 1st BASE Pte Ltd, Singapore) with -96 gIII sequencing primer (5'-<sup>HO</sup>CCC TCA TAG TTA GCG TAA CG -3', 10 pmol/μl).

### **Raman Spectroscopy**

HiPco SWCNTs dispersed by SDBS, 76-4 monomer, 76-4 dimer were filtrated using a membrane filter with a pore diameter of 0.025 μm, respectively. Raman spectra were recorded with a Renishaw Ramanscope in the backscattering configuration over several random spots on samples using laser excitation wavelength of 633 nm (1.96 eV), with laser intensity of 2.5 – 5 mW. G-band, D-band, and radial breathing mode (RBM) are clearly revealed on the normalized plots, demonstrating a typical behavior of SWCNT.

## Results

**Table S1.** Titering results of biopanning experiments for CNT-75-specific and CNT-76-specific phage eluates.

	CNT-75 (pfu/ $\mu$ l)	CNT-76 (pfu/ $\mu$ l)
1 <sup>st</sup> round (0.1% TBST)	$1.36 \times 10^4$	$4.60 \times 10^4$
2 <sup>nd</sup> round (0.2% TBST)	$3.55 \times 10^4$	$1.13 \times 10^5$
3 <sup>rd</sup> round (0.3% TBST)	$4.30 \times 10^4$	$1.83 \times 10^5$
4 <sup>th</sup> round (0.4% TBST)	$1.33 \times 10^5$	$2.70 \times 10^5$
5 <sup>th</sup> round (0.5% TBST)	$2.30 \times 10^5$	$3.20 \times 10^5$
6 <sup>th</sup> round (0.75% TBST)	$2.52 \times 10^5$	$7.20 \times 10^5$

**Table S2.** Individual amino acid frequency of CNT-75-specific pool in percent. Large relative changes (>100.0%) compared with the overall library distribution are highlighted. Negative signs indicate decreasing trend.

Amino Acid	CNT-75	Lib. Avg.	Change	Relative Change
A	5.4	6.0	-0.6	-10.7
C	0	0.5	-0.5	-100.0
D	0	2.8	-2.8	-100.0
E	0.6	3.1	-2.5	-80.8
F	2.4	3.3	-0.9	-27.8
G	3.6	2.6	1.0	37.4
H	13.7	6.3	7.4	117.3
I	2.4	3.4	-1.0	-30.0
K	4.2	2.8	1.4	48.8
L	3.6	9.3	-5.7	-61.6
M	3.0	2.6	0.4	14.5
N	1.8	4.6	-2.8	-61.2
P	14.9	12.2	2.7	22.0
Q	5.4	5.1	0.3	5.0
R	4.2	4.7	-0.5	-11.3
S	16.1	10.0	6.1	60.7
T	4.2	11.1	-6.9	-62.5
V	3.0	3.9	-0.9	-23.7
W	9.5	2.2	7.3	332.9
Y	2.4	3.6	-1.2	-33.9

**Table S3.** Individual amino acid frequency of CNT-76-specific pool in percent. Large relative changes (>100.0%) compared with the overall library distribution are highlighted. Negative signs indicate decreasing trend.

Amino Acid	CNT-75	Lib. Avg.	Change	Relative Change
A	2.8	6.0	-3.2	-53.7
C	0	0.5	-0.5	-100.0
D	0.6	2.8	-2.2	-80.2
E	3.9	3.1	0.8	25.4
F	5.0	3.3	1.7	51.5
G	0.6	2.6	-2.0	-78.6
H	13.9	6.3	7.6	120.5
I	1.7	3.4	-1.7	-51.0
K	0	2.8	-2.8	-100.0
L	5.6	9.3	-3.7	-40.3
M	3.9	2.6	1.3	49.6
N	1.7	4.6	-2.9	-63.8
P	11.7	12.2	-0.5	-4.4
Q	6.7	5.1	1.6	30.7
R	2.8	4.7	-1.9	-40.9
S	13.9	10.0	3.9	38.9
T	6.1	11.1	-5.0	-44.9
V	1.1	3.9	-2.8	-71.5
W	10.0	2.2	7.8	354.5
Y	8.3	3.6	4.7	131.5

**Table S4.** General amino acid grouping for statistical analysis.

Grouping	Amino Acids
Hydrophobic	A, G, I, L, V, M
(+) Charged	K, R
(-) Charged	D, E
Hydroxyl	S, T
Ring groups	F, Y, W, H
Amide groups	N, Q
Proline	P
Cysteine	C

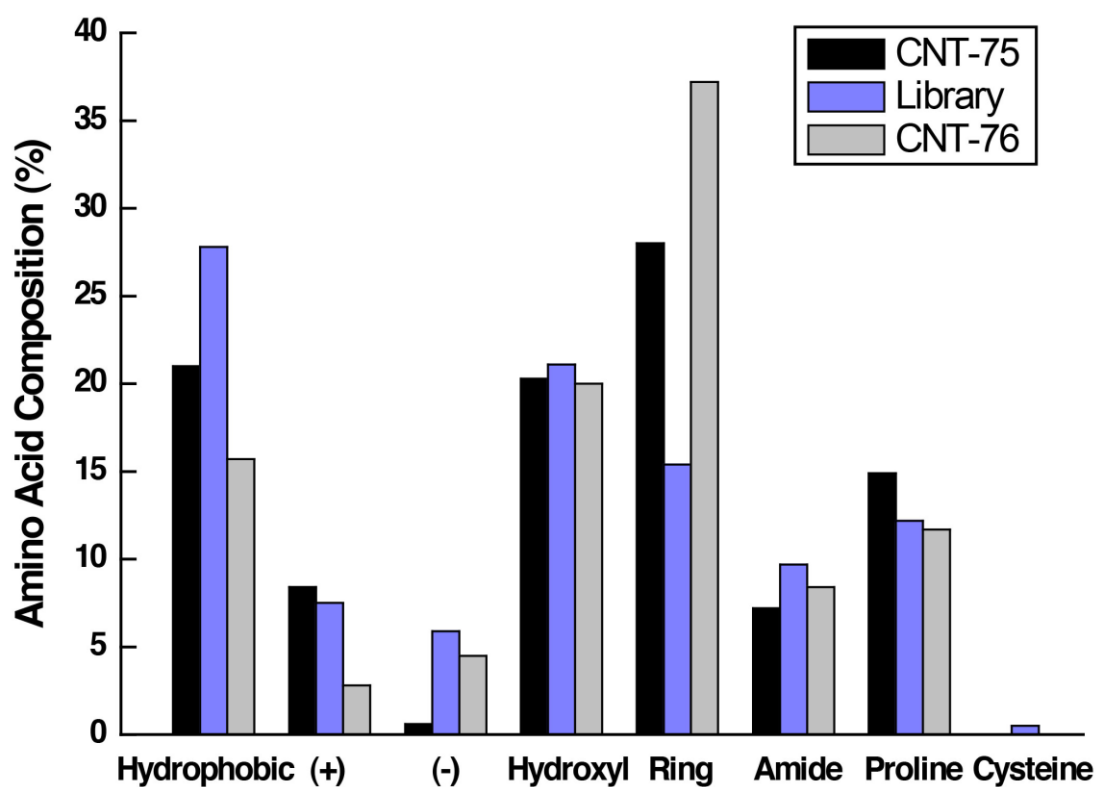


**Figure S1.** Amino acid grouping frequency of CNT-75-specific pool, Ph.D.-12 library and CNT-76-specific pool.

**Table S5.** The hydrophobicity of each amino acid and the average hydrophobicity of each CNT-75-specific sequence.

No.*	Hydrophobicity												Avg. Hydrophobicity
	1	2	3	4	5	6	7	8	9	11	11	12	
75-1	-0.5	0.23	-0.04	0.12	-0.48	-0.8	-1.38	-1.3	-1.36	-1.72	-1.04	-0.36	-0.72
75-2	-0.5	-0.2	-0.52	-0.38	-0.38	-0.66	-0.12	-0.34	-0.38	-0.54	-0.18	-0.78	-0.42
75-3	-2.5	-0.83	-1.86	-1.46	-1.42	-1.36	-0.62	0.06	0.06	0.02	-0.04	-0.1	-0.84
75-4	-0.5	-1.3	-0.84	-0.68	0.6	0.66	0.52	0.62	0.6	0.6	0.54	0.64	0.12
75-5	-1.8	-1.53	-0.96	-0.96	-0.6	-0.46	-0.3	-0.46	-0.06	0.1	0.06	0	-0.58
75-6	-0.5	-0.23	-1.32	-1.18	-1.6	-1.44	-0.94	-0.26	-0.24	0.04	-0.02	-0.02	-0.64
75-7	-1.8	-0.6	-0.44	-0.18	0.42	0.34	1.08	0.48	0.28	-0.42	-0.34	-0.4	-0.13
75-8	-0.5	-0.3	-0.22	-0.38	0.3	-0.56	-0.68	-0.54	-0.38	-0.38	-0.12	-0.04	-0.32
75-9	0.3	-0.3	-0.48	-0.8	0.1	0.04	0.4	0.4	1.26	0.66	0.66	0.6	0.24
75-10	-0.5	0.03	-0.62	-0.62	-0.68	-1	-1.14	-0.76	-0.76	-0.16	0.1	0.2	-0.49
75-11	-0.5	0.93	-0.62	-0.98	-1.94	-2	-1.6	-0.88	-0.36	-0.46	-0.46	-0.36	-0.77
75-12	-0.5	0.03	-1.12	-1.38	-1.4	-1.56	-1.38	-0.92	-0.56	-0.96	-0.86	-0.36	-0.91

\* The corresponding peptide sequences are HKLATSPWWPI (75-1), HSTSYQSLRWGA (75-2), FPPWWHNSSGAP (75-3), HWGNHSHKSHPQR (75-4), IYAHSLANSHNS (75-5), HSAFWQISPPST (75-6), LPPWKHKTSOVA (75-7), HWRQTMPMTSAP (75-8), SVSVGMPKSPRP (75-9), HSSQWHPMAVHR (75-10), HESFWYLPHQSY (75-11), and HSSWYIQHFPPL (75-12).

**Table S6.** The hydrophobicity of each amino acid and the average hydrophobicity of each CNT-76-specific sequence.

No.*	Hydrophobicity												Avg. Hydrophobicity
	1	2	3	4	5	6	7	8	9	11	11	12	
76-1	-0.5	0.03	-1.12	-1.38	-1.4	-1.56	-1.38	-0.92	-0.56	-0.96	-0.86	-0.36	-0.91
76-2	-0.5	-1.9	-1.68	-1.52	-1.26	-0.58	-0.58	-0.42	-0.48	-0.46	-0.46	-0.38	-0.85
76-3	-0.5	-0.23	-0.36	0.34	0.16	-0.34	0.22	0.48	-0.8	-1.04	-0.58	-1.18	-0.32
76-4	-0.5	0	-0.08	-0.28	-0.34	-0.32	0.36	-0.92	-0.58	-0.94	-1	-1	-0.47
76-5	-0.5	-0.73	-0.32	-0.9	-1.5	-1.34	-1.4	-1.56	-0.98	-0.38	-0.28	-0.28	-0.85
76-6	-0.5	0.93	-0.62	-0.98	-1.94	-2	-1.6	-0.88	-0.36	-0.46	-0.46	-0.36	-0.77
76-7	-0.5	0.9	-0.08	0.08	-0.64	-0.64	0.64	0.48	0.34	1.02	0.42	-0.18	0.15
76-8	-0.5	-0.3	-0.22	-0.38	0.3	-0.56	-0.68	-0.54	-0.38	-0.38	-0.12	-0.04	-0.32

\* The corresponding peptide sequences are HSSWYIQHFPPL (76-01), HLWTYSAPTVP (76-02), HTQNMRMYEPWF (76-03), HSNWRVPSPWQL (76-04), HTMSSWWAGHAT (76-05), HESFWYLPHQSY (76-06), HNRWSSWDEHTP (76-07), and HWRQTMPMTSAP (76-08).

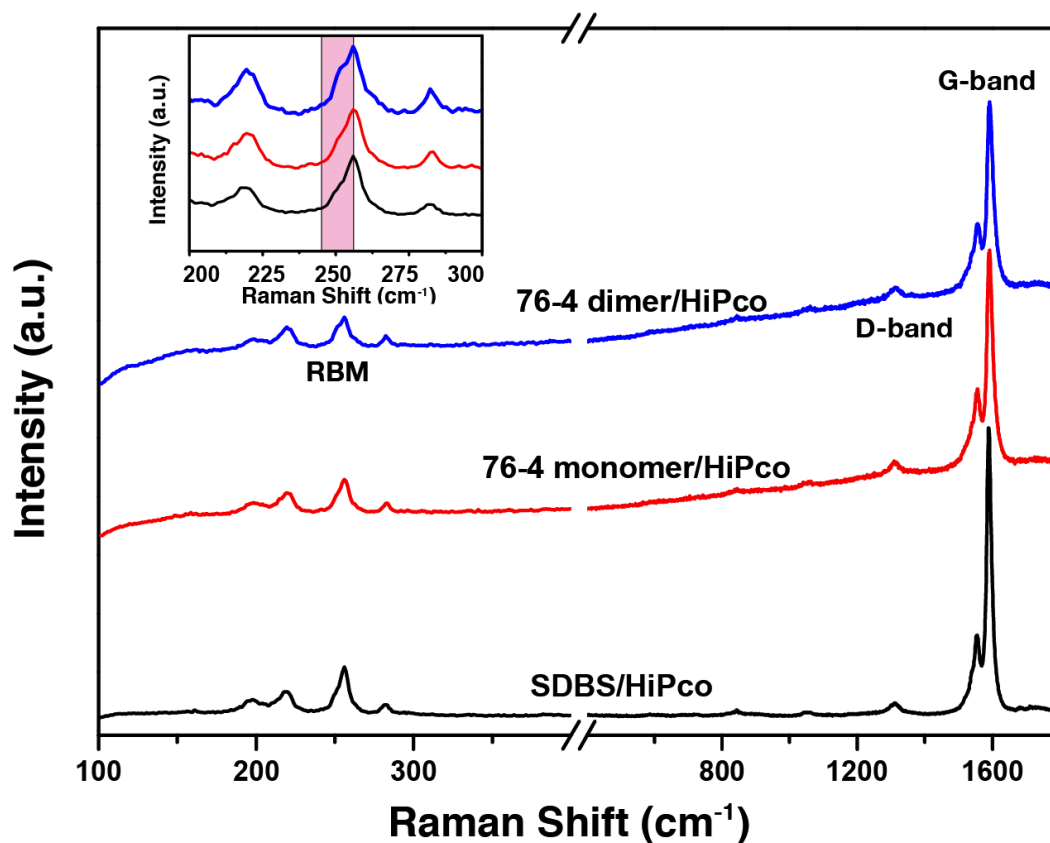


**Figure S2.** Raman Spectra of SWCNTs dispersed by SDBS, 76-4 monomer, and 76-4 dimer at 633 nm excitation. The G-band signals are normalized to the strongest peak. The inset shows the magnified RBMs and the region of new minor shoulders is highlighted in pink.

No difference is observed on G-band in the SWCNTs dispersed by peptides from the SWCNTs dispersed by SDBS, indicating that the selected peptides are not effective for metallic/semiconducting SWCNT separation. The intensity of D-band of peptide-dispersed SWCNTs is the same as that of SDBS-dispersed SWCNT. It confirms that the selected peptides non-covalently bind to SWCNTs and introduce no defects to their surface when dispersing SWCNTs. The shape of RBM peak of peptide-dispersed SWCNTs located around 250  $\text{cm}^{-1}$  is slightly altered and new minor shoulders appear on that peak. The change can be attributed to the preferential dispersion of large-diameter SWCNTs, such as (9, 5), (10, 3), and (12, 2), and verifies the results from fluorescence spectroscopy.